RSC Advances

PAPER

View Article Online
View Journal | View Issue

Cite this: *RSC Adv.*, 2020, **10**, 37545

Tunable electrical properties of carbon dot doped photo-responsive azobenzene–clay nanocomposites†

Jahnabi Gogoi, Shubham Shishodia and Devasish Chowdhury *

The development of photo-responsive nanocomposite materials is important in the fabrication of optoelectronic devices. In this work, we fabricated a carbon dot doped azobenzene–clay nanocomposite which possesses different ac conductivity with and without UV treatment. At first, azobenzene nanoclusters were synthesised and then successfully used to make an azobenzene–clay nanocomposite. It was observed that there is a small change in the ac conductivity of the azobenzene–clay nanocomposite with and without UV treatment. However, this change in ac photoconductivity can be enhanced in the azobenzene–clay nanocomposite by doping with electron-rich cysteine and methionine carbon dots. Hence, ac conductivity properties of the carbon-doped azobenzene–clay nanocomposite can be tuned using UV light. Impedance measurements were determined using Electrochemical Impedance Spectroscopy. Mechanistic insight into the phenomenon is also discussed in the paper. Thus fabrication of tunable carbon dot doped photo-responsive azobenzene–clay nanocomposites will lead to the use of carbon dot doped azobenzene–clay nanocomposites in photo-switchable optoelectronic devices.

Received 28th August 2020
Accepted 28th September 2020

DOI: 10.1039/d0ra07386e

rsc.li/rsc-advances

Introduction

There is a need to study the photophysical properties of new photosensitive materials so that these materials can be used as photoswitches and thus expand their use for applications in biology, materials science, and beyond. Photo-switchable molecules have the advantages of transformation into different states in different light conditions, stability in states and fast response which imparts a wide range of properties to these molecules.[1] And these advantages in the light-driven molecular transformations have consequently found their applications in photoswitches,[2] optical storage,[3] photodetectors,[4] phototransistors,[5] telecommunications,[6] photorefractive,[7] electro optics,[8] to name a few. Of the many photochromic or photosensitive molecules, azobenzene is extensively used in hybrid composition with various other materials for their use in energy-related applications.

Azobenzene is one of the well-known organic photosensitive molecules which can isomerise into *trans* and *cis* form based on the irradiation conditions. It has two phenyl rings which are separated by an azo bond (–N=N–).[9] Both these states are obtained under different conditions of light, which means it isomerises into *trans* to *cis* form under UV illumination and from *cis* to *trans* form under visible light.[10] The reversibility of the isomerised states is facilitated by the azo bond as this conjugated system show strong electronic absorption.[11] And as such, the electronic tunability around this conjugated system can be tuned to operate differently under UV light and visible light. Both these forms are different in their stability as the *trans* form is more stable thermodynamically than its *cis* form. Also, they differ in their planarity with the *trans* form assuming a planar form with C_{2h} symmetry and the *cis* form assuming a non-planar form with C_2 symmetry.[12] As such, the photo-responsive azobenzene has been used in incorporation with polymeric materials,[13,14] different nanostructured materials[15,16] and metal–organic frameworks[17–19] for energy storage applications.

The additional advantageous property of organic molecules facilitates variation in doping which is in turn facilitated by the molecular transformations in the presence of light. Azobenzene belonging to this category of organic molecules also have been used for similar purposes with modulated doping and dopant behaviour. The most favourable way to control the properties of the nanoscale materials is through doping.[20] Doping of carbon nanomaterials with heteroatoms causes a change in their

Material Nanochemistry Laboratory, Physical Sciences Division, Institute of Advanced Study in Science and Technology, Paschim Boragaon, Garchuk, Guwahati, 781035, India. E-mail: devasish@iasst.gov.in; Fax: +91 361 2279909; Tel: +91 361 2912073

† Electronic supplementary information (ESI) available: DLS size of AZO_{NC}, stacked PL spectra of azonanocluster with and without UV light, stacked PL spectra of methionine and cysteine nanoparticle, FTIR spectra of clay (BTN), Tauc plot, Electrochemical Impedance Spectroscopy of azonanocluster clay composite with and without UV at different input voltage, log *Z versus* log *f* plot of AZO_{NC}/Meth/BTN and AZO_{NC}/Cys/BTN with UV treatment at different response time. See DOI: 10.1039/d0ra07386e

tunable properties.[21] Incorporation of dopants in semiconductor nanostructured materials causes a change in their electronic structure, leading to changes in the optical and electrical behaviour of the materials, eventually making them suitable for such applications.[22] With wide-ranged properties of conductivity, carbon nanomaterials like graphene and carbon nanotubes are used in composition with azobenzene for various such applications. Not much work has been done in this area, but with the photo-switchable behaviour and the flexible property of doping, they have been used to form a hybrid composite with carbon nanomaterials. Peimyoo *et al.* showed the doping behaviour of the two isomerised forms of azobenzene on graphene using Raman Spectroscopy. Further, they studied the modulated doping behaviour under controlled light conditions, and it showed that the conformation changes with the doping affect the electronic properties of graphene.[23] In another work, Kim *et al.* showed non-covalent latching of azobenzene to graphene, and reversible photo-switchable behaviour of azobenzene led to light-controlled conductance modulation as well as modulated doping which attributed to the formation of improved light-gated transistors.[24] Zhang *et al.* on the other hand showed that the rapidly reversible isomerisation of the azobenzene under irradiation and its hybrid with graphene oxide having an internal short-ranged order led to its application as a highly sensitive photoswitch.[25] In the efforts to store clean, renewable solar energy in reversible molecular bonds, Kolpak *et al.* showed the usage of an azobenzene functionalised with carbon nanotubes with a volumetric density of Li-ion batteries for the construction of a novel recyclable, thermally stable solar fuel cell.[26] Chen *et al.* in their work investigated for the first time the electrochemical behaviour of hybrid composite reversible self-assembled graphene with azobenzene modified by surfactant and showed the light-induced polarity change electrochemical behaviour of the hybrids.[27] Owing to the conducting property of graphene and carbon nanotubes, Simmons *et al.* demonstrated the change in the conductivity of the carbon nanotubes in composite with azobenzene owing to the photoisomerisation behaviour of the azobenzene molecule.[28] Light-driven reversible isomerisation property of the azobenzene molecule had been used for the composition of photo controlled reversible conducting devices made of polymer and MWCNT hybrid composites with azobenzene.[29]

All of the reports show the use of nanostructures in hybrid composition with azobenzene, where the photoisomerisation behaviour of azobenzene facilitates doping as well as conductance change in graphene and the nanotubes. Also, all of these works shows the use of azobenzene molecule or functionalised azobenzene. Deka *et al.* in their work synthesized an azobenzene nanocluster retaining the photoisomerisation behaviour and this in composition with graphene and functionalised graphene showed the formation of a p-type and n-type nanocluster and its use as in electronic device.[30] Herein, we have also made an azobenzene cluster in composition with clay, which has a structural similarity with graphene and methionine and cysteine nanoparticles as dopants for modulation of the conducting properties of the system.

In this work, we have successfully synthesized a nanocluster from commercially available azobenzene through a simple hydrothermal method as per already established protocol by Deka *et al.*[30] The azobenzene nanocluster (AZO_{NC}) shows green fluorescence under UV light and is easily dispersed in aqueous media. The AZO_{NC} was further utilised to prepare azobenzene nanocluster–clay nanocomposite (AZO_{NC}/BTN). The AZO_{NC} was used in the nanocomposite to impart the photosensitized property of AZO_{NC}. There are various reports on the hybrid composition of azobenzene and graphene achieved by doping the graphene with azobenzene for use in different light-driven applications. To enhance the photo-tuning of the electrical properties, we doped the azobenzene nanocluster–clay nanocomposite (AZO_{NC}/BTN) with electron-rich species of methionine and cysteine nanoparticles. It was observed that the ac conductivity properties of doped nanocomposite could be tuned using UV light. Thus fabrication of tunable nanocomposite will lead to the development of photo-switchable devices.

Experimental section

Chemicals used

Azobenzene (98%) was purchased from Sigma-Aldrich, and sodium hydroxide pellets (Merck, India) were used while synthesising the azobenzene nanocluster. Bentonite clay (BTN) used in the synthesis of the nanocomposite was purchased from Sigma Aldrich, India. All the chemicals were used as obtained without further purification. The water used in all the experiments was from Milli-Q water purification system.

Characterisation

The prepared nanocomposites were characterised using the UV-visible spectroscopy on a Shimadzu 2600 UV-vis spectrophotometer to study the changes in absorbance of the nanocomposites and the starting materials. Fluorescence spectra were collected on a Jasco Spectrofluorometer (FP-8300). Fourier transform infrared studies were done using a Nicolet-6700 FTIR spectrophotometer. Particle size and zeta potential measurements were carried out using a Malvern Zetasizer Nanoseries, Nano-ZS90. Sonicator from Hwashin Technology was used for the sonication of samples. Furthermore, the impedance measurements were done using an electrochemical workstation CH instrument 660E.

Methodology

Synthesising azobenzene nanocluster (AZO_{NC})

Following the bottom-up synthesis approach, 1 g of azobenzene was taken in a beaker and melted. To this molten azobenzene, 20 ml of 0.1 M aqueous NaOH solution was poured. The mixture was sonicated for 30 min and then filtered. The filtrate was collected in a beaker and then it was centrifuged to obtain the azobenzene nanocluster dispersion in water.

Preparation of AZO_{NC}–clay nanocomposite (AZO_{NC}/BTN)

The nanocomposite was obtained by dispersing 0.3 g of bentonite (BTN) clay in 20 ml of as-synthesised azobenzene nanocluster. The mixture was then sonicated in a bath sonicator for 24 hours. Sonication was done here for exfoliating the dispersed BTN clay. After sonication, the obtained solution was then further mixed by using a Spinix shaker for 20 minutes. The sonicated and well-dispersed solution obtained from the above method was then collected for further characterisation.

Synthesising methionine carbon dots (CD-Meth)

1 g of L-methionine was taken in a beaker and heated at 280 °C for melting. The L-methionine turned black. To this, 30 ml of NaOH (10 mg ml^{-1}) was added. The solution mixture was sonicated for half an hour, it was filtered, and then the filtrate was centrifuged for 20 min at 10 000 rpm to obtain the methionine nanoparticles dispersed in water.

Preparation of AZO_{NC}–methionine–clay nanocomposite (AZO_{NC}/Meth/BTN)

1 : 2 ratio of AZO_{NC} and methionine carbon dot was mixed with 0.04 g of bentonite clay, and the mixture is kept for sonication for 24 hours. After sonication, the obtained solution was then further mixed by using a Spinix shaker for 20 minutes. The sonicated and well-dispersed solution obtained from the above method was then collected.

Synthesising cysteine carbon dots (CD-Cys)

1 g of L-cysteine hydrochloride monohydrate was taken in a beaker and heated at 240 °C for melting. The white powdery substance slowly turned to a brown sticky liquid (melt). To this hot mix, 30 ml of NaOH (10 mg ml^{-1}) was added. The solution mixture was then sonicated, filtered and the filtrate was centrifuged at 10 000 rpm for 20 min to obtain the cysteine nanoparticles dispersed in water.

Preparation of AZO_{NC}–cysteine–clay nanocomposite (AZO_{NC}/Cys/BTN)

AZO_{NC} and cysteine carbon dot was mixed in the 1 : 1 ratio. To this mixture, 0.04 g of clay was added, andthe mixture was kept for sonication for 24 hours. After sonication, the obtained solution was then further mixed by using a Spinix shaker for 20 minutes. The sonicated and well-dispersed solution obtained from the above method was then collected.

Deposition of nanocomposite on silicon wafer

By adopting the drop-cast method; we deposited the as-synthesised nanocomposite on a silicon wafer and kept it in an oven to dry for 12 hours. The resultant drop cast silicon wafer was then further characterised for potential electrical and photocatalytic applications. Before deposition, the silicon wafer was rinsed in 0.1 M HCl solution.

Results and discussion

In this work, a tunable electrical property of photosensitised nanocomposite demonstrated. Scheme 1 depicts the schematics of the protocol applied to fabricate a tunable doped photosensitised nanocomposite. At first azobenzene nanoclusters (AZO_{NC}) were prepared from azobenzene by the method developed and reported by our laboratory.[30] Further, the azobenzene nanoclusters were immobilised on clay to form azobenzene–clay nanocomposite (AZO_{NC}/BTN). The prepared azobenzene–clay nanocomposite (AZO_{NC}/BTN) demonstrated photosensitised property. It was observed that UV treated azobenzene–clay nanocomposite (AZO_{NC}/BTN) when drop cast on silicon wafer surface show lower ac conductivity than non-

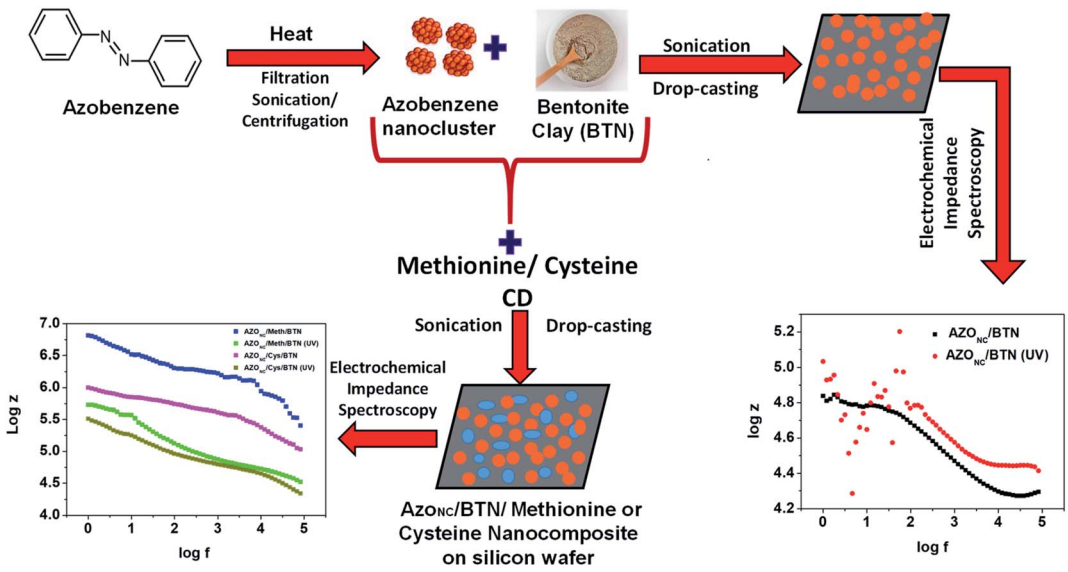

Scheme 1 Schematic representation of the protocol adopted for the preparation of the azobenzene–clay composites and their electrochemical impedance spectroscopy studies.

treated azobenzene–clay nanocomposite. However, the difference in the ac conductivity of UV treated and non-treated azobenzene–clay nanocomposite can be further enhanced with doping with methionine or cysteine carbon dots to form azobenzene–methionine–clay (AZO_{NC}/Meth/BTN) or azobenzene–cysteine–clay nanocomposite (AZO_{NC}/Cys/BTN). The ac conductivity measurements of the different azobenzene–clay nanocomposite were determined by Electrochemical Impedance Spectroscopy (EIS). Thus through doping tunable electrical property can be achieved of the photosensitized azobenzene–clay nanocomposite.

First azobenzene nanocluster (AZO_{NC}) was prepared as given in the experimental section. AZO_{NC} show fluorescence when viewed under UV light. Fig. 1S(A) in ESI† shows that photograph of AZO_{NC} in normal light and UV light. The AZO_{NC} show greenish fluorescence in UV. The dynamic light scattering (DLS) measurement show that the size of the $AZO_{NC} \sim 2$ nm (Fig. 1S(B) in ESI†). The photoluminescence (PL) properties of AZO_{NC} was also studied before and after UV treatment. The stacked PL spectra of azobenzene nanocluster, as shown in Fig. 1S(C)† in is obtained after exciting the nanocluster in the wavelength range of 300–410 nm. Initially, on excitation, the fluorescence intensity decreases but with further excitation, it increases to give the maximum emission at 450 nm at an excitation wavelength of 410 nm. The PL intensity is excitation dependent, and with a gradual increase in the excitation wavelength, the emission wavelength also shifts. The change in PL intensity is in accordance as per the earlier reports of carbon nanomaterials.[31] Similarly, the stacked PL spectra for the azobenzene nanocluster after exposer to UV light was also obtained (Fig. 1S(D)†). From the PL spectra, we observe that it follows the same trend as before. With the increase in excitation wavelength, there is first gradual decrease and then increase in the fluorescence intensity to give the maximum emission at 410 nm.

The carbon dots were then prepared from methionine and cysteine using the already established protocol developed by our laboratory. In this work methionine and cysteine was used as a doping agent to fabricate AZO_{NC}/Meth/BTN and AZO_{NC}/Cys/BTN nanocomposite. The stacked PL spectra for methionine and cysteine carbon dots were also obtained and is shown in the ESI Fig. 2S(A) and (B).† Both the methionine and cysteine carbon dots also shows excitation dependent fluorescence intensity. On excitation, the fluorescence intensity initially increases to reach the emission maximum at the excitation wavelength of 340 nm. On a further increase of the excitation wavelength, the intensity gradually decreases. The stacked PL spectra were obtained after excitation of the carbon dots in the wavelength range of 300–400 nm. Cysteine carbon dots were also characterised using photoluminescence spectroscopy in the wavelength range of 300–430 nm. Here also, the carbon dots

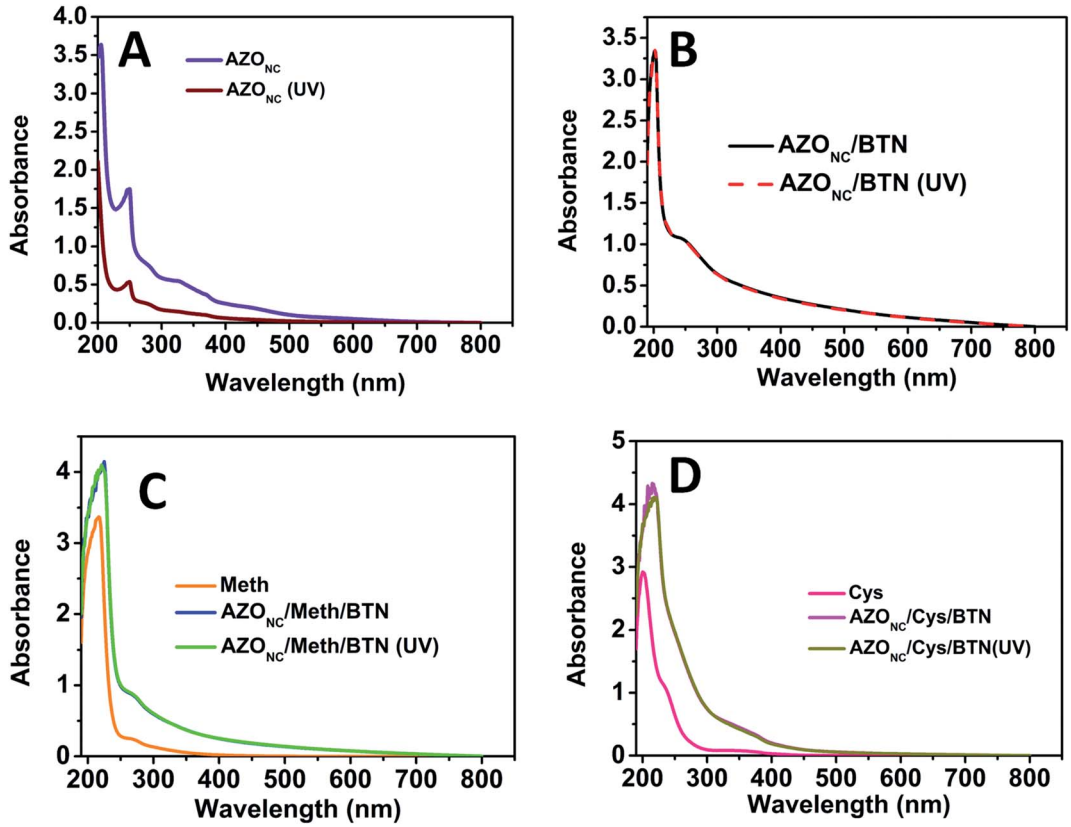

Fig. 1 Stacked UV-vis spectra of (A) azonanocluster (AZO_{NC}) with and without UV illumination, (B) composite of azonanocluster with clay (AZO_{NC}/BTN) with and without UV illumination, (C) methionine (Meth) and the composite of methionine with azonanocluster and clay with and without UV illumination and (D) cysteine (Cys) and composite of cysteine with azonanocluster and clay with and without UV illumination.

show excitation dependent PL intensity. The fluorescence intensity gradually increases with the increase in the excitation wavelength to obtain the maximum emission at the excitation wavelength of 410 nm. After that, with further increase in the excitation wavelength, the intensity decreases. The excitation dependent PL properties in carbon nanomaterials may arise due to surface defects, quantum confinement effects and defects in symmetry, and the exact mechanism operating behind these properties have not yet been understood.

The various azobenzene–clay nanocomposite prepared were subjected to different characterisation techniques like UV-vis Spectroscopy, Fourier Transformed Infrared Spectroscopy (FTIR), Scanning Electron Microscopy (SEM), Transmission Electron Microscopy (TEM), Photoluminescence Spectroscopy. Fig. 1 shows the UV-visible spectra of different azobenzene–clay nanocomposite *viz.* AZO_{NC}, AZO_{NC}/BTN, AZO_{NC}/Meth/BTN and AZO_{NC}/Cys/BTN in a stacked form under two different conditions of normal light and UV light illumination. Fig. 1(A) shows the UV-visible spectra of the AZO_{NC} in the presence of the UV light and absence of the UV light. In the spectra, we observe a sharp peak at 244 nm for AZO_{NC} and a slightly shifted peak at 250 nm for the AZO_{NC} system when illuminated with UV light. These peaks can be attributed to the π–π* transition due to the presence of –C=C– bond in the nanocluster. A broad peak at 325 nm has been observed for the AZO_{NC} possibly for n–π* transition that indicates the presence of the –N=N– bond in the azonanocluster.[30] However, AZO_{NC}/BTN does not show any change in the UV-visible spectrum when AZO_{NC}/BTN is exposed to UV (Fig. 1(B)). However, the peak looks very different when compared with AZO_{NC}.

It is observed from the spectrum that only one broad peak exist at about 250 nm. The characteristic absorbance peak for bentonite clay (BTN) observed at 248 nm, and disappearance of the peaks of the AZO_{NC} and appearance of broad peak proves the presence of an interaction between the AZO_{NC} and BTN and suggests the formation of a nanocomposite. Fig. 1(C) and (D) show the UV-visible spectrum of AZO_{NC}/Meth/BTN and AZO_{NC}/Cys/BTN, respectively, with and without UV irradiation. Also stacked and compared with UV-visible spectrum of Meth and Cys NPs. We observe a broad low-intensity peak at around 270 nm in AZO_{NC}/Meth/BTN, which might be due to n–σ* transition, which indicates the presence of –OH group in the compound. Similarly, FTIR analysis was carried out on all different azo–clay nanocomposite prepared. Fig. 2 shows the stacked FTIR spectra of the starting material azo nanocluster (AZO_{NC}), AZO_{NC}/BTN, methionine (Meth), cysteine (Cys) and their corresponding nanocomposite, *i.e.* AZO_{NC}/Meth/BTN and AZO_{NC}/Cys/BTN. From the FTIR Spectroscopy, few peaks that could be recognised are 3624 cm^{-1} for AZO_{NC} and AZO_{NC}/BTN nanocomposite, a broad peak at 3414 cm^{-1} for AZO_{NC}/Meth/BTN and a peak at 3436 cm^{-1} for AZO_{NC}/Cys/BTN. All the peaks correspond to O–H stretching. Similarly, the peak of AZO_{NC} found in 1443 cm^{-1} is due to the N=N stretching vibration.

This peak was slighted shifted at 1428 cm^{-1} for AZO_{NC}/BTN, at 1465 cm^{-1} for AZO_{NC}/Meth/BTN and at 1473 cm^{-1} for AZO_{NC}/Cys/BTN which indicates some interaction of N=N of AZO_{NC} after the formation of AZO_{NC}/BTN or AZO_{NC}/Meth/BTN or AZO_{NC}/Cys/BTN nanocomposite. The FTIR spectrum of BTN is provided in ESI Fig. 3S.† Apart from the similarity of the peaks of the hybrid composites with those of the corresponding peaks of clay (BTN) and AZO_{NC}/BTN, the nanocomposites prepared with doped methionine and cysteine nanoparticles also retain the characteristic peaks of methionine and cysteine nanoparticles respectively. The peak at 1577 cm^{-1} for methionine nanoparticles is also observed at a slightly shifted position of 1590 cm^{-1} for the AZO_{NC}/Meth/BTN composite system which might be due to the –N–H– bending vibration of the amino acid system. Similar peak position was also observed at 1625 cm^{-1} for cysteine nanoparticles and a shifted peak at 1587 cm^{-1} for its corresponding nanocomposite AZO_{NC}/Cys/BTN. The –OH stretching frequency around 3369 cm^{-1} for methionine and 3446 cm^{-1} for cysteine respectively are also retained in the nanocomposites with a slight change in the peak positions present at 3414 cm^{-1} for AZO_{NC}/Meth/BTN and to 3436 cm^{-1} for AZO_{NC}/Cys/BTN nanocomposite. FTIR of BTN also taken and shown in ESI Fig. 3S.† It can be observed that the peak at 3449 cm^{-1} corresponding to the presence of O–H depicting that BTN is rich in –OH functionality.

The surface morphology of AZO_{NC}/BTN, AZO_{NC}/Meth/BTN and AZO_{NC}/Cys/BTN was studied using Scanning Electron Microscopy (SEM). Fig. 3(A)–(C) shows the representative SEM images of AZO_{NC}/BTN, AZO_{NC}/Meth/BTN and AZO_{NC}/Cys/BTN, respectively. The images clearly show the surface morphology. However, no nanoparticle is visible on the surface of the nanocomposite, which indicates that doped nanoparticles are embedded in the nanocomposite. The nanoparticles in the composite can be seen in the representative transmission electron microscope images. Fig. 3(D) shows the visible clustered azobenzene in its nano form. Similarly, carbon dots of methionine and cysteine can also be seen in the carbon dot doped systems AZO_{NC}/Meth/BTN and AZO_{NC}/Cys/BTN (Fig. 3(E) and (F)).

Band-gap energy

The optical band gaps of different azobenzene nanocomposite were estimated using empirical formula

$$(\alpha h\nu)^2 = A(h\nu - E_g) \quad (1)$$

where A is a constant that depends on the transition probability, E_g is the optical band gap energy, h is the Plank constant and ν is the frequency. The E_g of different azobenzene nanocomposite were calculated by extrapolating a straight line to the $(\alpha h\nu)^2 = 0$ axis in the plots of the $(\alpha h\nu)^2$ *versus* optical band gap energy. Assuming that the transition probability was 1, the equation could be simplified as

$$(\alpha h\nu)^2 = h\nu - E_g \quad (2)$$

The Tauc plot for determining the energy gap of AZO_{NC}/BTN is shown in Fig. 4S.† The energy gap of AZO_{NC}/BTN is determined to be 4.08 eV. Similarly, Tauc plot was drawn for AZO_{NC}/

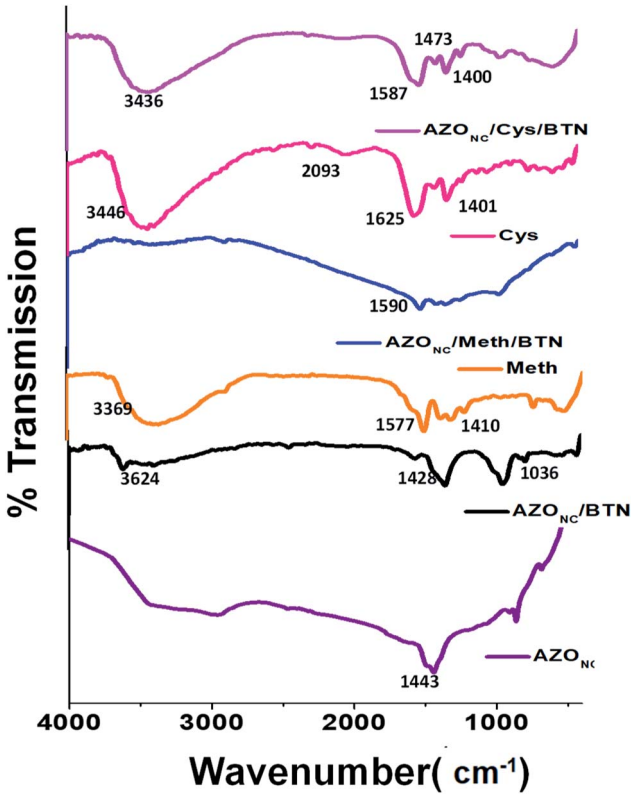

Fig. 2 The stacked FTIR spectra of azobenzene nanocluster (AZO_{NC}), azobenzene nanocluster with clay (AZO_{NC}/BTN), methionine (Meth), azobenzene nanocluster and clay composite with methionine (AZO_{NC}/Meth/BTN), cysteine (Cys) and azobenzene nanocluster and clay composite with cysteine (AZO_{NC}/Cys/BTN).

Meth/BTN and AZO_{NC}/Cys/BTN. Fig. 5S(A) and (B) in ESI† shows that Tauc plot for AZO_{NC}/Meth/BTN in the presence of normal light and after treatment with UV light respectively. From the plot, the energy gap was determined to be 3.82 eV, and with UV treatment drops to 3.76 eV. Fig. 5S(C) and (D) in ESI† shows that Tauc plot for AZO_{NC}/Cys/BTN in the presence of normal light and after treatment with UV light respectively. From the plot,the energy gap was determined to be 3.91 eV,and with UV treatment drops to 3.81 eV.

Conductivity studies

The prepared nanocomposite systems were then tested for their electrical conductivities using Electrochemical Impedance Spectroscopy (EIS) under two different conditions of normal light and the UV light of 365 nm. The illumination was carried out using a UV lamp (JSGW, India). EIS requires to perform by sweeping through a wide range of frequencies at a single perturbation amplitude. EIS uses small perturbations rather small potential sweeps and steps in case of other electrochemical measurements such as cyclic voltammetry or chronoamperometry. Since we have used a photosensitised material azobenzene nanocluster as the starting material in preparing the nanocomposites and this photosensitised material behaves differently under the different conditions of normal light and UV light. Moreover, the photo-switchable property of the azobenzene has also retained in azobenzene nanocluster so, the photo-switchable property of the azobenzene in different nanocomposite systems has been explored by studying its response to an applied voltage at a particularly perturbed amplitude in a wide range of frequencies.

In the first study, the electrochemical impedance curves of the azobenzene–clay nanocomposite was observed at a different frequency range of 1 Hz to 10^5 Hz and an amplitude of 0.005 V as a part of a two-electrode system to standardise the system. Fig. 6S in ESI† shows the response of the azobenzene–clay nanocomposite with clay at a range of input voltage from ±1 V to ±0.001 V. Fig. 6S(A)† shows the response of the hybrid system at different voltages under ordinary room conditions. Fig. 6S(B)† shows the response of the same composite system at different voltages under the UV illumination. It can be observed that under UV illumination, the nanocomposite does not show much difference in their conducting behaviour as compared to that of the composite behaviour under normal light conditions. However, the only change that we observe from the graph is that, with increasing input voltage, the resistivity of the system decreases and thus, a change in conductivity is observed. Hence, the further ac conductivity measurements were noted in the particular input voltage of 1 V. The comparative plot of log Z *vs.* log f at an amplitude of 0.005 and input voltage of 1 V is shown in ESI Fig. 7S.† It shows that change in ac impedance; hence the conductivity behaviour is not vastly different under normal light and UV light condition. It needs to be mentioned here that log Z *vs.* log f as measured in ac impedance studies is a measure of the change in impedance (Z) with frequency. The decrease in log Z *vs.* log f plot in a system signifies decrease of impedance and hence increase in ac conductivity of the system.

Further, EIS measurement was carried out on doped nanocomposite, *i.e.* AZO_{NC}/Meth/BTN and AZO_{NC}/Cys/BTN. Fig. 4 shows log Z *vs.* log f of AZO_{NC}/Meth/BTN and AZO_{NC}/Cys/BTN in normal light as well as after UV illumination. It is evident from Fig. 4(A) and (B) there is observed visible change in the

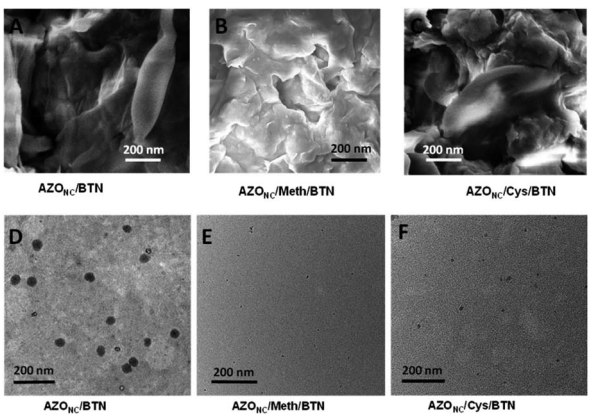

Fig. 3 Scanning electron microscope image of (A) AZO_{NC}/BTN, (B) AZO_{NC}/Meth/BTN and (C) AZO_{NC}/Cys/BTN; transmission electron microscope of (D) AZO_{NC}/BTN, (E) AZO_{NC}/Meth/BTN and (F) AZO_{NC}/Cys/BTN.

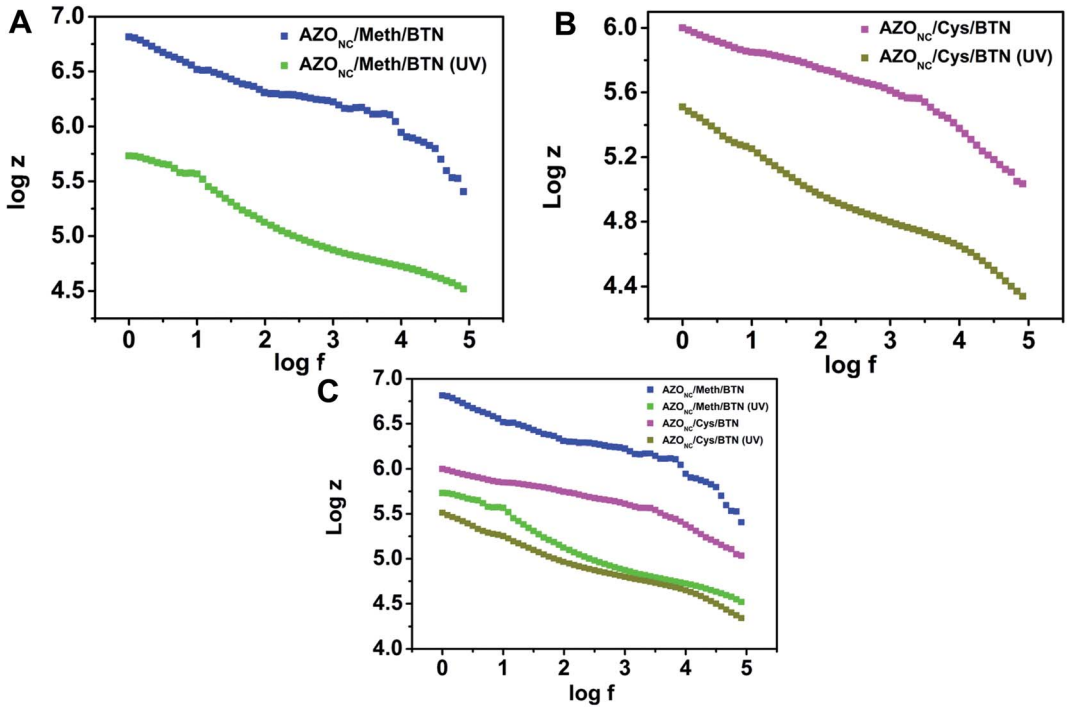

Fig. 4 log *Z versus* log *f* plot of (A) AZO_{NC}/Meth/BTN with and without UV treatment (B) AZO_{NC}/Cys/BTN with and without UV treatment and (C) comparative plot of (A) and (B).

conducting properties of the nanocomposite after doping with electron-rich moiety Meth CDs and Cys CDs. Here we observe that under the application of UV light, the resistivity of the AZO_{NC}/Meth/BTN and AZO_{NC}/Cys/BTN nanocomposite system decreases and thus, the conductivity of the systems increases. These doped nanocomposite systems of AZO_{NC}/Meth/BTN and AZO_{NC}/Cys/BTN were subjected to time varied EIS study under UV illumination to see the response of the composites at different time variations. Fig. 8S(A) and (B) in ESI† shows the response of the composite systems through the plot of log *Z vs.* log *f* under similar conditions of amplitude and input voltage. The only variation is time. The change in ac impedance study was conducted at the time variations of 5 min, 10 min, 15 min and 20 min of UV illumination. The AZO_{NC}/Meth/BTN composite system had approximately the same response irrespective of the time of UV illumination. However, in the case of AZO_{NC}/Cys/BTN, the system had slightly different conductance behaviour with illumination time. The variation is maximum at 20 min, so EIS measurement of carbon dot doped system was taken at 20 min.

Fig. 4(C) gives us a comparative insight into both AZO_{NC}/Meth/BTN and AZO_{NC}/Cys/BTN nanocomposite system. The comparative plot demonstrates that methionine doped nanocomposite system has higher conductivity than the cysteine doped composite system under similar conditions (UV treatment). The comparative plot demonstrates that photoswitching of conductivity of AZO_{NC}/BTN can be enhanced by doping with Meth NPs and Cys NPs. All the measurements were carried out in amplitude 0.005 and input voltage at 1 V.The photoswitchable property observed in AZO_{NC}/Meth/BTN, and AZO_{NC}/Cys/BTN nanocomposite is due to the presence of photosensitized material AZO_{NC}. The statement is justified by the fact that methionine–clay and cysteine–clay nanocomposite does not show any change in ac conductivity under similar condition. Fig. 5 shows the log *Z vs.* log *f* plot of methionine–clay nanocomposite under normal light and UV illumination. The plot clearly shows that there is no change is ac conductivity under two different condition. This proves the importance of azobenzene as a photo-switchable material in the fabrication of such nanocomposite. In this work, we have used a photosensitising molecule that responds to light and have shown the effect of doping with an electron rich system and therefore the change in conductivity of the nanocomposite system owing to the light controlled changes in the photosensitiser molecule alone. Reports in literature show the use of similar photosensitiser molecules in a nanocomposite system with different

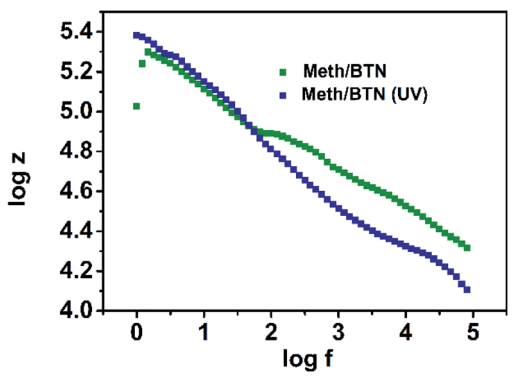

Fig. 5 log *Z versus* log *f* plot of methionine–clay nanocomposite with and without UV treatment.

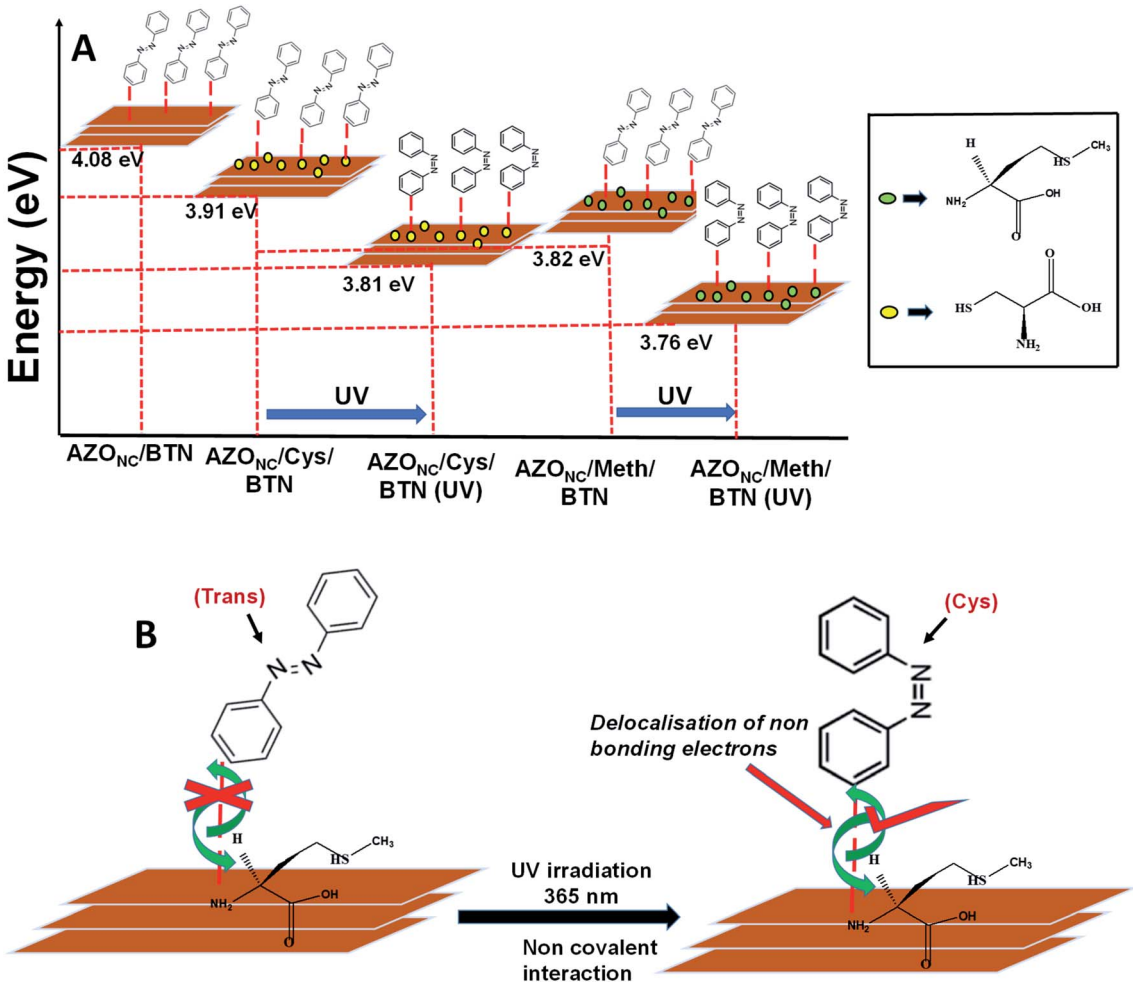

Fig. 6 (A) Energy level diagram of AZO$_{NC}$/BTN, AZO$_{NC}$/Meth/BTN, AZO$_{NC}$/Cys/BTN with and without UV treatment. (B) Schematic representation of possible interaction of *cis* and *trans*-AZO$_{NC}$ with Meth and Cys CDs.

systems such as graphene, multiwalled carbon nanotubes, polymeric systems.[23–29] Also there are reports of nanocomposite systems that comprises of polymeric films incorporating different nanoparticles which have shown change in conductance properties (ac and dc) of the nanocomposite system.[32,33] But the changes in the conductivity of those systems are in accordance with the increase and decrease of wt% of the nanoparticles into the systems with an already conducting polymeric material. In case of the nanocomposite systems of graphene, single walled carbon nanotube, multiwalled carbon nanotube, polymers that used a photosensitiser molecule similar to the one that we have used, azobenzene, all of the reports suggest change in the conductance properties of the systems owing to the interaction of the azobenzene with an already conducting system such as graphene and carbon nanotubes. But in our work we have used the photosensitising molecule to dope with electron rich species and have further seen the conductance switching of the nanocomposite owing to the interaction of the photosensitiser molecule with the dopants under visible and UV light conditions. Given below is a comparative table of nanocomposite systems that have been discussed in literature that shows switching of conductance behaviour in different conditions (Table 1).

Mechanistic insight into the phenomena

We tried to understand the mechanism behind the enhanced ac conductivity of doped azobenzene–clay nanocomposite. It is well known that the *trans* form of azobenzene exists in a planar form, and its *cis* form exists in the non-planar arrangement. Similarly, in its nanocluster form also, we have shown earlier that azobenzene retains its planarity in *trans* form and non-planarity in *cis* form. In other words, azobenzene nanoclusters inherit the photo-isomerisation property.[24] We had shown earlier that azobenzene immobilised in graphene oxide sheet, *trans*-azobenzene nanocluster over these graphene-based systems stacking is taking place between the two parallel aromatic ring system, p orbital overlap is maximum. Hence there is more delocalisation of the electrons. As a result, there is increased conductivity in case of *trans*-GO AZO$_{NC}$. On the other hand, upon the photo-isomerisation to the non-planar *cis* form, the p-orbital overlap decreases, and so does the conductivity.

Table 1 Comparative nanocomposites systems in literature with tunable electrical conductivity behaviour

Nanocomposite system	Doping	Conductance behaviour	Importance	Reference
Azobenzene–graphene system	Methyl orange doped on graphene	Photocontrolled	Use of graphene as a molecular transformation probe	23
Azobenzene–graphene system	Azobenzene	Photocontrolled	High levels of doping with reversible doping in graphene	24
DR1 functionalised single walled carbon nano tube	Anthracene	Photocontrolled	Successful noncovalent functionalisation of nanotube transistors	28
MWCNT–polymer nanocomposites	Azobenzene embedded in PMMA	Photocontrolled	Photoswitching with stable amplitude	29
Polyaniline–NiO nanocomposites	NiO nanoparticles	Wt% of nanoparticles	Composition based tunable conductivity	32
Dopamine–polypyrrole nanostructures	None	DA–Ppy mole ratios	Composition based applications of the nanocomposites	33
Azobenzene–clay nanocomposite	Methionine and cysteine CD'S	Photocontrolled	Light controlled Tunable conductivity of azobenzene in nanoform with variation in the dopant	Present work

Here unlike graphene oxide, clay although planar does not have an aromatic ring-based system. So, the different photo-isomerised form of AZO_{NC} immobilised in the clay system, the planarity and orientation do not have a substantial effect on the conductivity properties of the system under different isomerisation conditions. However, it is observed that there is a considerable change in the conductivity under normal light and UV light upon doping with methionine (Meth CDs) and cysteine carbon dot (Cys CDs.) The change in conductivity is because azobenzene nanocluster and doped Meth CDs and Cys CDs have substantial interaction. The two phenyl rings of azobenzene with a –N=N– bond has delocalised π electrons as well as non-bonding electrons. These π electrons and non-bonding electrons interact with those of the methionine and cysteine. This interaction between the two systems is facilitated more in the *cis* state of the azobenzene molecule, and hence after UV treatment, the conductivity of that system increases. Also, we know that the length of the conjugation system determines the extent of delocalisation and as the conjugation increases, the energy gap between the valence band and the conduction band also decreases resulting in better flow of electrons between the two systems. As such, the conductivity of the system is also larger. Methionine with a longer parent carbon chain is assumed to have a more extensive conjugated system than cysteine. Furthermore, as such the delocalisation of electrons in the azobenzene clay methionine system is more than azobenzene clay cysteine system. Hence the better conductivity results in the former case upon reversible photo-controlled condition (Fig. 6).

Conclusion

In summary, photo-responsive material like azobenzene was used to fabricate UV responsive photoconductive nanocomposite. First, azobenzene nanoclusters were synthesised, followed by azobenzene–clay nanocomposite. It was observed that there is a small change in ac conductivity of azobenzene–clay nanocomposite with and without UV treatment.

However, this change in ac photoconductivity can be distinctly enhanced in azobenzene–clay nanocomposite by doping with cysteine and methionine carbon dots. Hence, ac conductivity properties of carbon-doped azobenzene–clay nanocomposite can be tuned using UV light. The bandgap calculation also indicates that ac conductivity of cysteine and methionine carbon dots azobenzene–clay nanocomposite: AZO_{NC}/Meth/BTN and AZO_{NC}/Cys/BTN, decrease when treated with UV. The impedance measurements were determined using Electrochemical Impedance Spectroscopy. The photo-responsive behaviour observed by carbon dot doped azobenzene clay nanocomposite was due to the presence of azobenzene nanoclusters. This is confirmed as carbon dot doped clay nanocomposite did not show photo-conductive behaviour. The two phenyl rings of azobenzene with a –N=N– bond has delocalised π electrons as well as non-bonding electrons has strong interaction with electrons of the methionine and cysteine. This interaction between the two systems is facilitated more in the *cis* state of the azobenzene molecule. Hence the doped AZO_{NC}/Meth/BTN and AZO_{NC}/Cys/BTN nanocomposite after UV treatment show lower and enhanced ac conductivity. Thus, tunable carbon dot doped photo-responsive azobenzene–clay nanocomposites are potential material for its application in photo-switchable optoelectronic devices.

Conflicts of interest

There are no conflicts to declare.

Acknowledgements

JG wants to thank IASST for fellowship. The authors thank the Central Instrumentation Facility (CIF) of IASST for instrumentation facility.

Notes and references

1 B. Y. Choi, S. J. Kahng, S. Kim, H. Kim, H. W. Kim, Y. J. Song, J. Ihm and Y. Kuk, *Phys. Rev. Lett.*, 2006, **96**, 156106.
2 M. Del Valle, R. Gutierrez, C. Tejedor and G. Cuniberti, *Nat. Nanotechnol.*, 2007, **2**, 176–179.
3 A. R. Yuvaraj, Md. L. Rahman and M. M. Yusoff, *Int. J. Spectrosc.*, 2016, 1–9.
4 X. Zhou, T. Zifer, B. M. Wong, K. L. Krafcik, F. Leonard and A. L. Vance, *Nano Lett.*, 2009, **9**, 1028–1033.
5 N. Guo, L. Xiao, F. Gong, M. Luo, F. Wang, Y. Jia, H. Chang, J. Liu, Q. Li, Y. Wu, Y. Wang, C. Shan, Y. Xu, P. Zhou and W. Hu, *Adv. Sci.*, 2019, 1901637, DOI: 10.1002/advs.201901637.
6 D. Zhou, R. Piron, M. Dontabactouny, O. Dehaese, F. Grillot, T. Batte, K. Tavernier, J. Even and S. Loualiche, *Appl. Phys. Lett.*, 2009, **94**, 081107.
7 K. Meerholz, B. L. Volodin, Sandalphon, B. Kippelen and N. Peyghambarian, *Nature*, 1994, **371**, 497–500.
8 M. Lee, H. E. Katz, C. Erben, D. M. Gill, P. Gopalan, J. D. Heber and D. J. Mcgee, *Science*, 2002, **298**, 1401–1403.
9 A. A. Beharry and G. A. Woolley, *Chem. Soc. Rev.*, 2011, **40**, 4422–4437.
10 O. Sadovski, A. A. Beharry, F. Zhang and G. A. Woolley, *Angew. Chem., Int. Ed.*, 2009, **48**, 1484–1486.
11 C. J. Barrett, J. Mamiya, K. G. Yagerc and T. Ikeda, *Soft Matter*, 2007, **3**, 1249–1261.
12 M. Bockmann, N. L. Doltsinis and D. Marx, *Phys. Rev. E*, 2008, **78**, 036101.
13 E. Blasco, B. V. K. J. Schmidt, C. Barner-Kowollik, M. Pinol and L. Oriol, *Macromolecules*, 2014, **47**, 3693–3700.
14 F. D. Jochum, L. Z. Borg, P. J. Roth and P. Theato, *Macromolecules*, 2009, **42**, 7854–7862.
15 D. Samanta, J. Gemen, Z. Chu, Y. Diskin-Posner, L. J. W. Shimon and R. Klajn, *Proc. Natl. Acad. Sci. U. S. A.*, 2018, **115**, 9379–9384.
16 C. L. Jones, A. J. Tansell and T. L. Easun, *J. Mater. Chem. A*, 2016, **4**, 6714–6723.
17 R. Lyndon, K. Konstas, B. P. Ladewig, P. D. Southon, P. C. J. Kepert and M. R. Hill, *Angew. Chem., Int. Ed.*, 2013, **52**, 3695–3698.
18 Y. Zhu and W. Zhang, *Chem. Sci.*, 2014, **5**, 4957–4961.
19 G. Das, T. Prakasam, M. A. Addicoat, S. K. Sharma, F. Ravaux, R. Mathew, M. Baias, R. Jagannathan, M. A. Olson and A. Trabolsi, *J. Am. Chem. Soc.*, 2019, **141**, 19078–19087.
20 D. Mocatta, G. Cohen, J. Schattner, O. Millo, E. Rabani and U. Banin, *Science*, 2011, **332**, 77–81.
21 M. K. Barman, B. Jana, S. Bhattacharyya and A. Patra, *J. Phys. Chem. C*, 2014, **118**, 20034–20041.
22 X. Dong, D. Fu, W. Fang, Y. Shi, P. Chen and L. J. Li, *Small*, 2009, **5**, 1422–1426.
23 N. Peimyoo, J. Li, J. Shang, X. Shen, C. Qui, L. Xie, W. Huang and T. Yu, *ACS Nano*, 2012, **6**, 8878–8886.
24 M. Kim, N. S. Safron, C. Huang, M. S. Arnold and P. Gopalan, *Nano Lett.*, 2012, **12**, 182–187.
25 X. Zhang, Y. Feng, P. Lv, Y. Shen and W. Feng, *Langmuir*, 2010, **26**, 18508–18511.
26 A. M. Kolpak and J. C. Grossman, *Nano Lett.*, 2011, **11**, 3156–3162.
27 S. Chen, L. Bao, E. Ou, C. Peng, W. Wang and W. Xu, *Nanoscale*, 2015, **7**, 19673–19686.
28 J. M. Simmons, I. In, V. E. Campbell, T. J. Mark, F. Leonard, P. Gopalan and M. A. Eriksson, *Phys. Rev. Lett.*, 2007, **98**, 086802.
29 S. W. Basuki, V. Schneider, T. Strunskus, M. Elbahri and F. Faupel, *ACS Appl. Mater. Interfaces*, 2015, **7**, 11257–11262.
30 M. J. Deka, S. K. Sahoo and D. Chowdhury, *J. Photochem. Photobiol., A*, 2019, **372**, 131–139.
31 B. Li, Y. Guo, A. Iqbal, Y. Dong, W. Li, W. Liua, W. Qin and Y. Wang, *RSC Adv.*, 2016, **6**, 107263–107269.
32 H. S. Roya, M. M. Islama, M. Y. A. Mollahband and M. A. B. Hasan Susana, *Mater. Today*, 2019, **15**, 380–387.
33 W. Zhang, Y. Zhou, K. Feng, J. Trinidad, A. Yu and B. Zhao, *Adv. Electron. Mater.*, 2015, **1**, 1500205.

